

Video Article

# In Situ Microscopy for Real-time Determination of Single-cell Morphology in Bioprocesses

Anna Maria Marbà-Ardébol<sup>1</sup>, Joern Emmerich<sup>1</sup>, Michael Muthig<sup>2</sup>, Peter Neubauer<sup>1</sup>, Stefan Junne<sup>1</sup>

<sup>1</sup>Chair of Bioprocess Engineering, Department of Biotechnology, Technische Universität Berlin

<sup>2</sup>SOPAT GmbH

Correspondence to: Stefan Junne at [stefan.junne@tu-berlin.de](mailto:stefan.junne@tu-berlin.de)

URL: <https://www.jove.com/video/57823>

DOI: [doi:10.3791/57823](https://doi.org/10.3791/57823)

Keywords: *In situ* microscopy, cell size, morphology, microbes, population heterogeneity, budding, growth vitality, agglomeration, monitoring, image detection

Date Published: 9/13/2018

Citation: Marbà-Ardébol, A.M., Emmerich, J., Muthig, M., Neubauer, P., Junne, S. *In Situ* Microscopy for Real-time Determination of Single-cell Morphology in Bioprocesses. *J. Vis. Exp.* (), e57823, doi:10.3791/57823 (2018).

## Abstract

*In situ* monitoring in microbial bioprocesses is mostly restricted to chemical and physical properties of the medium (e.g., pH value and the dissolved oxygen concentration). Nevertheless, the morphology of cells can be a suitable indicator for optimal conditions, since it changes with dependence on the growth state, product accumulation and cell stress. Furthermore, the single-cell size distribution provides not only information about the cultivation conditions, but also about the population heterogeneity. To gain such information, a photo-optical *in situ* microscopy device<sup>1</sup> was developed to enable the monitoring of the single-cell size distribution directly in the cell suspension in bioreactors. An automated image analysis is coupled to the microscopy based on a neural network model, which is trained with user-annotated images. Several parameters, which are gained from the captures of the microscope, are correlated to process relevant features of the cells, like their metabolic activity. Until now, the presented *in situ* microscopy probe series was applied to measure the pellet size in filamentous fungi suspensions. It was used to distinguish the single-cell size in microalgae cultivation and relate it to lipid accumulation. The shape of cellular particles was related to budding in yeast cultures. The microscopy analysis can be generally split into three steps: (i) image acquisition, (ii) particle identification, and (iii) data analysis, respectively. All steps have to be adapted to the organism, and therefore specific annotated information is required in order to achieve reliable results. The ability to monitor changes in cell morphology directly *in line* or *on line* (in a by-pass) enables real-time values for monitoring and control, in process development as well as in production scale. If the *off line* data correlates with the real-time data, the current tedious *off line* measurements with unknown influences on the cell size become needless.

## Introduction

Morphological features of cells are often related to the physiological state, a connection between form and function exists for many applications. The morphology of a single cell is influenced by the state of growth, the cell's age, osmotic and other potential cell stresses or product accumulation. Morphological changes of cells are often a measure of the growth vitality of a culture. Intracellular product synthesis, lipid accumulation in algae and inclusion body formation in bacteria, among others, are related with the cell size as well. Cell agglomeration can be another factor that is worth investigating as summarized recently<sup>2</sup>.

Population heterogeneities can be quantified based on morphological features of individual cells. Studies showed that heterogeneity within a culture might be significant, e.g., under large-scale production conditions<sup>3</sup> the overall yield might be affected by a low performance of subpopulations<sup>4</sup>.

Usually, the assessment of morphological features of cells is performed by manual sampling or with a by-pass flow chamber coupled to a photo-optical device. This leads to several restrictions: the limited amount of acquired data can hardly provide statistically reliable measurements; the time delay in between sampling and the accessibility of results may be too long in comparison to the dynamics of the process; and most important, the sampling procedure (location of the sampling port, pre-treatment of the sample before the measurement, unfavorable conditions in the sampling or bypass tube) can trigger a biased error as the sample procedure itself can already affect cell morphology. Finally, there exists always a high risk of contamination during sampling or in by-pass solutions, if they are not sterilizable in place.

The application of *in situ* microscopy (ISM) can circumvent several of these problems. If cells are detected automatically, a correct identification of their morphological features can be surveyed<sup>5</sup>. Until now, the main limitations of this method were (i) the evaluation time of images, which was too long for *in situ* applications, and (ii) the poor resolution of images, especially at high cell densities. Although first solutions of ISM included mechanical sampling, dilution of the probe, or were restricted to a by-pass system<sup>6,7</sup>, further approaches allow capture of the cell suspension directly<sup>8</sup>.

Recent advances in ISM allow for the *in line* or *on line* monitoring of cells on a single-cell basis, which provides the distribution of morphological parameters in real-time directly in cell suspensions at considerably high cell concentrations. Through *off line* analyses of the cells' key parameters, correlations with information provided by the coupled automated cell detection and ISM can be identified. Then, new soft sensor designs are achieved, in which an unmeasurable parameter is estimated with the single-cell morphology.

In this report, the ISM is conducted by coupling a photo-optical probe to an automated image analysis. The ISM consists of a single-rod sensor probe that enables the capture of images within a known focus range in an adjustable measurement gap with a high-resolution CCD camera [MM-Ho = CCD GT2750 (2750x2200) and MM 2.1 = CMOS G507c (2464x2056)]. The flash light illumination is conducted by transmission. Therefore, the light originates from the opposite side of the camera<sup>9</sup>. Cells pass continuously through this gap with the liquid flow. Hence, a representative sample population is obtained. The probe can be mounted directly to the bioreactor so that it reaches into the cell suspension, or it can be used in a sterilizable by-pass. The sensor shell is connected to the system prior to sterilization, the optical parts are afterwards mounted into the shell.

Until now, relevant industrial microorganisms, e.g., filamentous fungi (diameter of up to over 200  $\mu\text{m}$ ), the heterotrophic microalgae *Cryptocodinium cohnii* (average cell diameter of 20  $\mu\text{m}$ ), and the yeast *Saccharomyces cerevisiae* (average cell diameter of 5  $\mu\text{m}$ ), were investigated with this or similar devices, which is shortly described.

Filamentous fungi tend to form pellets under certain cultivation conditions. These are of a size of up to several hundred  $\mu\text{m}$ . The hyphae of the fungal cells develop different lengths in dependence to the hydrodynamic stress in the fluid phase. This has an influence on the metabolic and growth activity, substrate uptake and product release. ISM was applied to identify the pellet size distribution and the width of zones of lower biomass density at the edges of the pellets (own unpublished data).

The size of *C. cohnii* alters between 15 and 26  $\mu\text{m}$  when cells accumulate the polyunsaturated fatty acid docosahexaenoic acid (DHA) under nitrogen limitation. This biotechnological DHA production process consists of two parts, the growth phase, in which cells divide and become smaller, and the production phase, in which cells accumulate the product and thus become larger. Therefore, the cell size was used to determine the process state, in which either growth or DHA production was favorable. Finally, a correlation between the cell size and the DHA content was found. In this case, ISM allows to monitor the intracellular DHA accumulation in real time without the requirement of sampling, cell disruption, and the common gas chromatography analysis<sup>10</sup>.

Budding yeast is usually of a size between 3 and 8  $\mu\text{m}$ . The proportion of cells that are in the maturation state at a time, as described with the budding index (BI), provides information about the growth vitality<sup>11,12</sup>, and even a relation with recombinant protein secretion has been proven<sup>13</sup>. With the help of ISM, budding and non-budding yeast cells (cells with and without a bud) were distinguished<sup>14</sup>. Stress conditions can also lead to a broader variation of the cell size within a yeast population, as recently shown in scale-down cultivations, in which the conditions of large-scale nutrient-limited fed-batch cultivations were mimicked<sup>3</sup>.

Therefore, ISM has the potential to monitor growth vitality and product formation on a single-cell level during all stages of a bioprocess for the identification of optimal cultivation conditions, or for the purpose of process control. The methods described here are focused on microbial applications with single cells, but are also applicable to larger particles like human and animal cells, cell agglomerates and pellets of filamentous organisms.

## Protocol

NOTE: The following steps are necessary to adapt the parameters to the respective microorganism and culture conditions. The adjustment of probe settings lasts about 20 min for an experienced user. A detailed description of tools and steps is given in the corresponding manual. In general, the tools that are presented in the following protocol are needed: (i) *Probe Controller* for probe adjustments and image acquisition; (ii) *Fiji (ImageJ)* for annotations on acquired images; (iii) *SOPAT support* for artificial neural network (ANN) training and workflow creation; (iv) *Batcher* for data batch processing using already acquired images with a workflow; (v) *Result Analyzer* for result visualization and evaluation on batch processed images; and (vi) *Monitor* for automated real-time measurement and result visualization.

## 1. Setting Hardware Parameters

1. Prepare a culture with the highest cell concentration that might be achieved during the experiment or centrifuge and resuspend the pellet in order to achieve this concentration. In this case, choose 65 g L<sup>-1</sup> of dry biomass concentration for *S. cerevisiae* cultivations.
2. Prepare different dilutions, which range from the highest to the lowest concentration so that the expected range is fully covered. A minimum of 4 different concentrations are recommended.
3. Identify the cell size range of the microorganism with conventional microscopy. Define the expected maximum diameter ( $d_{\text{max}}$ ) of respective cells. This value is set to 8  $\mu\text{m}$  in case of *S. cerevisiae*.
4. Choose two measurement gaps of 5x and 10x of the expected  $d_{\text{max}}$  of the cells.
5. Choose the maximum stroboscope intensity. Choose stroboscope intensities for both gaps with the highest cell concentration so that cells are still visible on the images with the lowest light intensity (darkest images).
6. Choose the minimum stroboscope intensity, and then choose stroboscope intensities for both gaps so that cells are still visible on the images with the highest light intensity (brightest images). Use the lowest cell concentration, which likely appears during the measurement period.
7. Choose one focus position, which yields the sharpest images for each measurement gap, for both stroboscope intensities and for the concentration range that need to be tested (see step 2 for details about focusing). Focus cells appropriately so that the image data can be annotated afterwards (see step 4).
8. Measure the previously prepared dilution series of the cell concentration (see step 2) with both gap widths and stroboscope intensities.

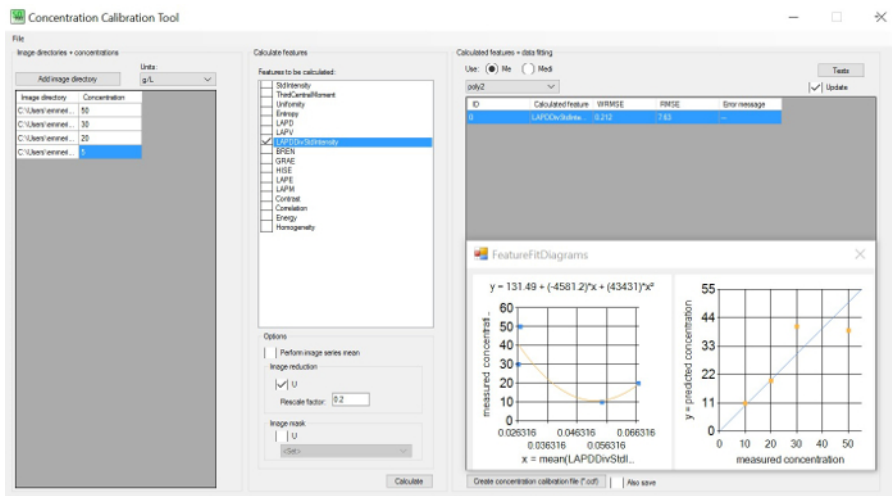


**Figure 1. Concentration calibration tool.** Left GUI: set image directories (minimum of 3) with known concentrations; central GUI: choose features to be calculated on the image directory; right GUI: choose the weighted root mean square error (WRMSE) to identify the minimum. WRMSE and the best correlation between any image feature and the cell concentration. [Please click here to view a larger version of this figure.](#)

9. Evaluate the dilution series experiment.
  1. Use the **Concentration Calibration (CoCa) Tool** (see **Figure 1**) to identify the optimal correlation between the extracted image features (brightness or sharpness) and the previously measured concentrations provided by the user, e.g., dry biomass or cell counts. Follow the instructions in the software manual for further details.
  2. Identify the optimal correlation between the extracted information from the image features at various concentrations compared to any *off line* measurements. See the legend of **Figure 1**.
  3. Choose the most reasonable measurement gap and stroboscope intensities under consideration of the concentration correlation curve with the features that result in the smallest weighted root mean square error (WRMSE).  
NOTE: The measurement gap is fixed during the experiment, whereas the stroboscope intensity can be adapted according to the cell concentration.

## 2. Off Line Measurement

1. Adjust the desired measurement gap according to step 1 with the help of a thickness gauge.
2. Open the graphical user interface **Probe Controller** in the dashboard.
3. Connect the desired probe to the amplifier in the software subsection **Actions** and press **Connect**.
4. Open the tab **Probe control** and adjust the desired stroboscope intensity according to step 1.
5. Press the **Play** button to start streaming (**Live View**).
6. Clean the measurement gap by spraying ethanol into the gap and carefully wipe any dust or dirt with an optical paper. Check that the glass of the sensor is free of particles with the **Live View** in the **CamControl**.  
NOTE: Particles and dust disturb measurements and the automatic cell identification.
7. Place a dry optical paper in the measurement gap and move the focus manually. Turn the binding screw until the single fibers of the paper are clearly seen.
8. Fill a tube with culture broth. Dip the microscope in the culture broth so that the gap is fully covered with cell suspension and focus on the cells by fine-tuning the focus binding screw. The focus must not be changed anymore during the experiment.  
NOTE: 5-6 mL of culture broth are added to a 50 mL conical centrifugal tube to float the measuring gap sufficiently.
9. Define the number of frames per time point [-] in the user interface in the menu **Triggering** in the GUI **Frames per trigger**. Set the number of frames to 200 frames per trigger.  
NOTE: The number of frames can be reduced to the lowest value, which is necessary for a statistical reliable result. This depends on the sample size required to obtain a representative morphological cell size distribution (see also step 5).
10. Define the frame rate [Hz] in the menu **Triggering** in the GUI **Frame rate**. Choose a frame rate that guarantees that moving particles from a previous frame will not appear in the following frame.  
NOTE: This can be proven with a test trigger with 200 frames. Inspect the images for particles, which are captured repeatedly. If this is the case, decrease the frame rate. For *off line* measurements, 1 Hz is recommended.
11. Set the directory, in which the acquired images will be saved, in the menu **General**.
12. Perform an image acquisition by activating the **Start image trigger acquisition** button. Move the tube with culture suspension gently up and down to induce a flow through the measuring gap.
13. Repeat step 2.6 after each measurement.
14. Check the acquired images. Cells have to be sharp enough for annotation. Inspect the images for particles, which are captured repeatedly. If this is the case, decrease the frame rate.
15. Save the settings by selecting the following pathway: C:\Program Files\SOPAT GmbH\monitoringPrograms\camcontrol, and press **Save**.

### 3. On Line (By-Pass) or In Line Measurement

1. Perform the *off line* measurement procedure first (see step 2) in order to set the hardware and software settings as a function of the organism and process (concentration or media).
2. Upload the saved settings from the previous section by selecting the button Load and select the following pathway: C:\Program Files\SOPAT GmbH\monitoringPrograms\camcontrol.
3. Connect the probe to the flow cell or to the bioreactor.  
NOTE: *In situ* measurements can be performed with a pinch flange.
4. Perform sterilization.  
NOTE: Only the probe-wetted material of the instrument is sterilizable through steam sterilization. The probe wetted length can go from 6 to 222 mm (Figure 2).

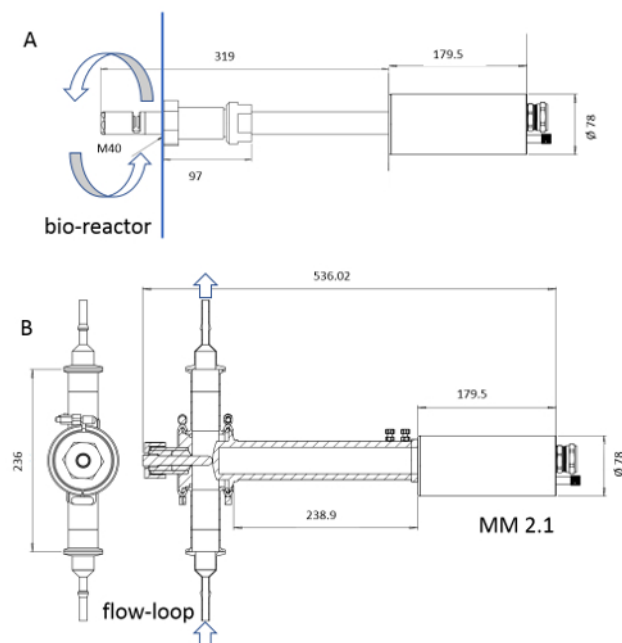


**Figure 2. Sketch of the ISM devices.** The probe MM-Ho (A) is installable directly in the bioreactor, whereas the probe MM 2.1 (B) can be used as a by-pass. The culture broth circulation is marked with arrows in each picture. The conversion factors are  $0.166 \mu\text{m pix}^{-1}$  for MM-Ho and  $0.087 \mu\text{m pix}^{-1}$  for MM 2.1. [Please click here to view a larger version of this figure.](#)

5. Define the image acquisition rate in the GUI **Triggering** in the field **Trigger interval [s]**.  
NOTE: Depending on the process dynamics, the image acquisition rate can be adapted. For example, if a lag-phase of 3 hours is expected, the rate of acquisition can be lower, than if a metabolism shift or the accumulation of a product shall be monitored. Usually, this requires a much shorter acquisition time in the minute range. For example, an image acquisition sequence between 5 and 10 min during a batch yeast cultivation provides sufficient information to capture process dynamics.
6. Define the frame rate as explained in step 2.10.  
NOTE: In *on line* and *in line* measurements, the frame rate can be increased, since the mechanical stirring can increase the flow rate through the gap.
7. Start image acquisition by activating the button **Start streaming of selected probe**.
8. Stop acquisition when the experiment is finished with the button **Stop streaming of selected probe**.  
NOTE: For the 1<sup>st</sup> run, start the acquisition just before the inoculation of the culture and proceed to step 4. For the following runs, open the program **Monitoring** in the dashboard and select the created workflow (see step 4). Start the monitoring just before the inoculation of the culture by pressing the **Play** button.

## 4. Particle Identification

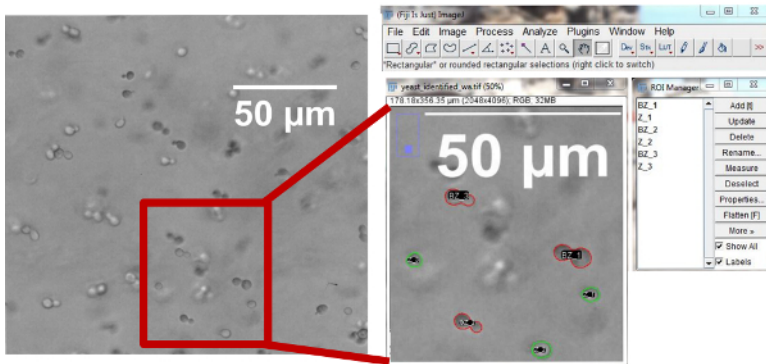


**Figure 3. Fiji tool user interface.** A training set is created with the annotated images. A manual annotation consisting of two classes is depicted, the list of annotated particles is shown in the ROI Manager. Different names and colors can be set for different classes. [Please click here to view a larger version of this figure.](#)

1. Annotate particles for the training of the artificial neural network (ANN) (training set).
  1. Load the acquired images into the annotation tool "**Fiji, ImageJ**" by dragging and dropping the file into the Main "**ImageJ**" window (see GUI "**Fiji**" tool in **Figure 3**)
  2. Open the ROI Manager by selecting: **Analyze | Tools | ROI Manager**.
  3. Choose a selection tool. **Wand (tracing) tool, freehand, oval, or elliptical** selections are recommended.
  4. Draw a circle around the particle that shall be annotated with the selection tools mentioned before and then refine it with the brush tool.
  5. Add the annotation to the **ROI Manager** by pressing **Add [t]**.
  6. Mark all objects of interest (cells to be identified) on about 15 images.  
NOTE: In order to cover all necessary information, *i.e.*, different shapes, sizes, concentration of cells, brightness, *etc.*, use five images from the start, five images from in between, and five images from the end of the experiment.
  7. Decide, if cells need to be classified in different subclasses due to their shape (*e.g.*, different phases of a cell cycle), or if all cells are of the same class.
  8. Change the name of each selected particles accordingly. Set one name or abbreviation for each class and a counter for each particle of the class (*e.g.*, cell\_1, cell\_2, *etc.*). Annotate at least 50 particles per class.
  9. Do not annotate objects, which should not be detected, because they are not relevant for the process, such as gas bubbles or other particles like undissolved media components.  
NOTE: Those events will not be included in the training procedure for the ANN and be regarded as background.
  10. Do not annotate cells that are out of focus.
  11. Annotate the images as consistent as possible. If there are doubts, the label **Ignore** can be applied. It is highly recommended not to abuse its use, since the ANN will only recognize structures that are labeled.
2. Save the annotated objects and the image to a ZIP format and send the file to the training network, either *via* upload to the platform or by sending the ZIP file *via* e-mail.  
NOTE: Usually, it takes a number of iterative training rounds to identify adequate predictions of the classified objects on the images. Each training round leads to a workflow that is returned by the program.
3. Use the workflow (\*.wf) with the trained object recognition algorithm to analyze test images with the data batch progressing program **Batcher** that can be started in the dashboard.
4. Check object detection on the test images through the quantification of false positive and negative events.
  1. Quantify the detection of false positive events: particles erroneously detected as cells, cells that are not correctly classified, and cells of which the contour has not been well identified.
  2. Quantify the false negative events (cells that are not recognized as such).
5. Visualize the results in the tool **Result analyzer** by starting the program in the dashboard.
  1. Import the desired results files with **File | Import file** or **File | Import folders**.
  2. Visualize the results by **Chart | Create chart** on the Charts GUI.
  3. Select one of the following options: Distribution chart, Sensitivity plot, Characteristic over time, Characteristic over survey points, and Feature vs. feature.  
NOTE: A manual regarding the utilization of the **Result Analyzer** comes with the system and is also available from the support.
  4. If the results are acceptable, run the workflow in the **Batcher** on all acquired images of the experiment. At the same time then the monitoring program can be created by combining the saved settings from the **Probe Controller** (\*.pcfg) with the workflow (\*.wf), see also the manual.  
NOTE: The workflow can also be used for monitoring future experiments for this culture media.
  5. If the results are not acceptable, check the annotation on the training set and/or continue with another iterative training round (see step 4.2).



## 5. Sample Size Quantification

1. Set the standard deviation ( $\sigma$ ), which is acceptable among the detected particles.  
NOTE: The standard deviation changes in parallel to the cell size homogeneity. The maximum standard deviation indicates the sample with the highest degree of size heterogeneity.
2. Set the amplitude of the confidence interval or the desired accuracy in relation to the expected variance of measurements.
3. Set the admitted error ( $\alpha$ ) between 5% ( $z_{1-\alpha/2} = 1.96$ ) and 10% ( $z_{1-\alpha/2} = 1.64$ ).
4. Calculate the number of cells to be identified from each class from equation 1.

$$n = \left( \frac{\sigma z_{1-\alpha/2}}{\epsilon} \right)^2 \quad \text{[Equation 1]}$$

NOTE: Based on the number of cells, the number of images that needs to be acquired can be defined for each data point.

5. Perform a sensitivity analysis on random time points of the experiment to check that the analysis of  $n$  particles leads to a variability of the mean Feret diameter and the  $Dv_{90}$  of less than 5%. It can be calculated automatically in the **Result Analyzer**.

## Representative Results

The cell size detection in yeast cultures with the ISM and automated image detection to distinguish between budding and non-budding cells was successfully conducted. Both the stroboscope intensity and the choice of the measurement gap have a range of tolerance, in which the particle identification is not affected. For example, *S. cerevisiae* cells were measured with various stroboscope intensities within a variation range of 11% at a dry biomass concentration of  $4 \text{ g L}^{-1}$ . The corresponding images provided sharp cell boundaries, therefore the particle identification was feasible with an acceptable variation of the cell size (1%) regardless of the stroboscope intensity. In case the stroboscope intensity is not properly adjusted, the images suffer from over-lighting and a proper cell identification will not be feasible (**Figure 4**).

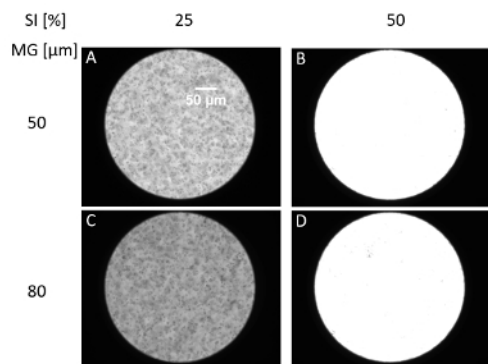


**Figure 4. Image acquisition features.** Examples of various stroboscope intensities (SI-%) and measurement gaps (MG-μm) for capturing *S. cerevisiae* cells (present values of SI and MG are indicated in brackets): **A** (25, 50); **B** (50, 50); **C** (25, 80); and **D** (50, 80). [Please click here to view a larger version of this figure.](#)

So far, the measuring gap cannot be re-adjusted during an *in situ* measurement. Therefore, the dilution series experiment is crucial in order to guarantee reliable data throughout a cultivation. The main concern is the occurrence of unidentifiable overlapping events due to the increment in cell concentration.

A sensitivity plot (sensitivity analysis of characteristic values, e.g., mean cell diameter with respect to particle number  $n$ ) of all detected cells from the loaded data file can be visualized (**Figure 5**). The user must decide which stability of a certain process parameter is needed. In this case the minimum number of cells needed for one valid data point. In consequence, more or less images can be analyzed for one data point.

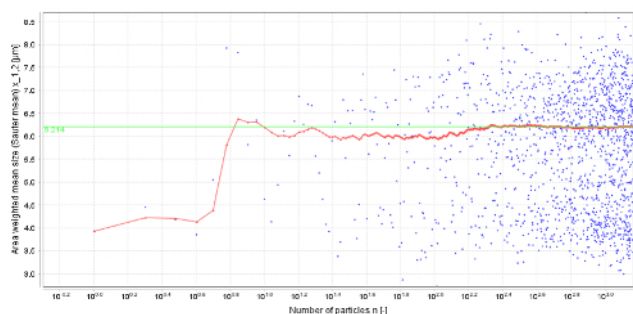


**Figure 5. Mean cell diameter sensitivity plot.** Variability of the mean cell diameter in dependence of the number of detected particles. A constant value of the mean cell diameter is achieved with about 1,000 cells. [Please click here to view a larger version of this figure.](#)

The annotation is the key point in order to achieve the desired accuracy of the particle identification. **Figure 6** shows an example of a "user annotation" (A), which is used as a training set for the neural network, as well as the particle identification on an image of the test set (unknown data for the neural network), which is used for its evaluation (B). Both images should have a similar rate of identified events.

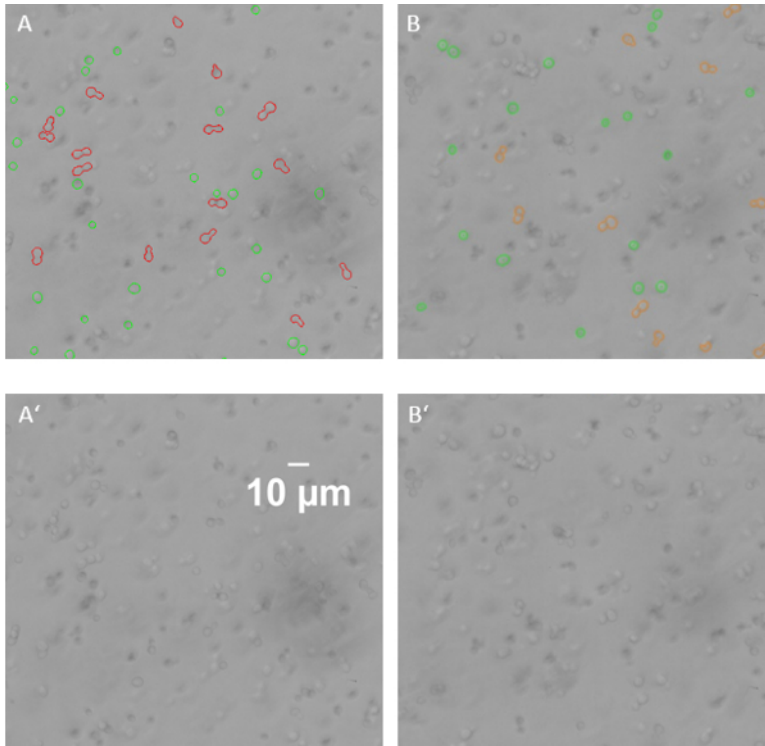


**Figure 6. Comparison of user annotation (training set) and automatic detection (test set).** Training set: annotated and original pictures are depicted in **A**, and **A'**, respectively. The information of this picture is used to train the ANN. Test set: the workflow created after training the ANN is applied to captures, which have not been used for the training: automatically identified cells (shown in **B**) from the original capture **B'**. [Please click here to view a larger version of this figure.](#)

As an example of the effect of intracellular product accumulation on the cell size distribution, the accumulation of the polyunsaturated fatty acid docosahexaenoic acid (DHA) by nitrogen limitation was investigated in the heterotrophic microalgae *C. cohnii*. It was demonstrated that the accumulation of the product can be quantitatively detected by means of ISM<sup>10</sup>. The method is currently used to investigate the impact of shear forces in stirred bioreactors on the morphological heterogeneity of cells.

The maturation state of the budding yeast *S. cerevisiae* was quantified. In the case of budding, the proportion of cells that are in the maturation state at a time (described with the BI), provides information of the growth activity and population heterogeneity. The automatic cell recognition was able to identify and distinguish budding and non-budding (or daughter) cells successfully in cell suspension<sup>15</sup>. The cell size distribution of three samples is shown in **Figure 7**. A shift to smaller cells indicates a lower portion of budding cells within the population.

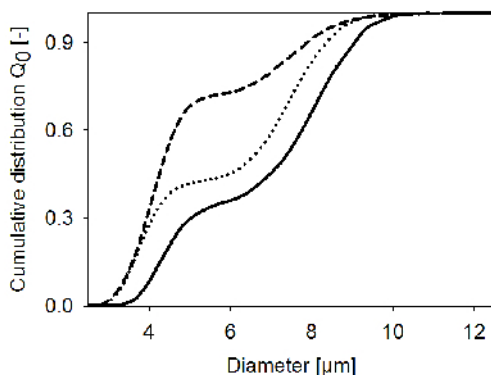


**Figure 7. Cumulative single-cell size distribution.** Cell size distributions measured during the time course of a cultivation at 3 h (straight line), 7 h (dotted line), and 13 h (dashed line). [Please click here to view a larger version of this figure.](#)

## Discussion

ISM as presented here with the same or very similar devices was used to measure morphologic dynamics of fungi, microalgae, and yeast cells, which enabled the determination of growth activity, and in case of algae, intracellular product accumulation. The sensor has no movable parts and is directly applicable in any standard stirred tank bioreactor, either through a standard port or in a sterilizable by-pass. Since yeast is much smaller than algae, the reduction in cell size required some recent hardware adaptations like a higher camera resolution and illumination

by transmission in order to get a sufficient pixel resolution of the yeast (for technical details, see<sup>15</sup>). However, there exists still a limitation for measuring even smaller cells like bacteria. The current *in situ* photo-optical instrumentation indicates limitations regarding overlapping particle information in high concentration and interference effects with structures below the UV/VIS spectrum. Up to date, image analysis algorithms for bacterial suspensions have not been applied, apart from brightness correlations<sup>16</sup>.

Other previously applied ISM tools were used to determine the cell concentration in order to show their reliability. This, however, became crucial if cells overlapped each other at elevated concentrations. Therefore, the focus of this study was not cell quantification, but morphological feature detection, while image features like brightness intensity can be correlated to the cell density as performed with other devices, too<sup>17</sup>. Otherwise all these devices would be limited to low cell concentrations; a maximal concentration of ca. 20 g L<sup>-1</sup> of yeast cells was evaluated when using a cell recognition approach vs. ca. 80 g L<sup>-1</sup> when using a cluster size algorithm.

In order to track the morphological features of a cell, its edges need to be detected accurately. In the case of algae, this is rather simple as the size changes, but the form remains constant throughout the transition of process stages. In contrast, yeast cells provide a bigger challenge due to their form, which cannot be approximated to a sphere or ellipse when cells are budding. Nevertheless, until now the cell size was calculated under the assumption that a cell is a perfect sphere in ISM measurements<sup>18</sup>. Although this approximation is close to the reality for some cases, more complicated forms such as budding cells or rod-shaped cells cannot be properly assessed. In this study, however, different forms were analyzed successfully due to the flexible boundary detection enabled through machine learning algorithms. Furthermore, overlapping events are still under investigation<sup>19</sup> to achieve a further development stage.

Currently, the gold standard for vitality and viability assessment is to count colony forming units or to stain a sample with a viability dye<sup>20</sup>, e.g., methylene blue or methylene violet<sup>21</sup>; however, this procedure can influence results. Whenever such features are related to the cell morphology<sup>22</sup>, the potential of rapidly assess them should be explored by the increasing potential of ISM. Furthermore, critical process parameters and/or quality attributes<sup>23</sup> can be related to shape, agglomeration and pellet formation, which all can be monitored by ISM.

Investigations with other key microorganisms frequently used in bioprocess are currently performed. The time for the adaptation of the object recognition algorithms and feature extraction for feature analysis depends mainly on the complexity of the images and the expected accuracy of the results. In the future, colored image capture will be considered in order to further broaden the range of information, which could be obtained on a single-cell level, e.g., if pigments are accumulated or in genetically modified organisms, in which colored markers were integrated.

## Disclosures

The authors have nothing to declare.

## Acknowledgements

The authors are thankful for the support of the German Federal Ministry of Economics and Energy within the framework ZIM-Koop, project "Smart Process Inspection", grant no. ZF 4184201CR5.

## References

- Maaß, S., Rojahn, J., Hänsch, R., Kraume, M. Automated drop detection using image analysis for online particle size monitoring in multiphase systems. *Computers & Chemical Engineering*. **45** 27-37 (2012).
- Lemoine, A., Delvigne, F., Bockisch, A., Neubauer, P., Junne, S. Tools for the determination of population heterogeneity caused by inhomogeneous cultivation conditions. *Journal of biotechnology*. **251** 84-93 (2017).
- Marbà-Ardébol, A. M., Bockisch, A., Neubauer, P., Junne, S. Sterol synthesis and cell size distribution under oscillatory growth conditions in *Saccharomyces cerevisiae*. scale-down cultivations. *Yeast*. **35** (2), 213-223 (2017).
- Xiao, Y., Bowen, C. H., Liu, D., Zhang, F. Exploiting nongenetic cell-to-cell variation for enhanced biosynthesis. *Nature chemical biology*. **12** (5), 339-344 (2016).
- Beutel, S., Henkel, S. In situ sensor techniques in modern bioprocess monitoring. *Applied microbiology and biotechnology*. **91** (6), 1493 (2011).
- Belini, V. L., Wiedemann, P., Suhr, H. In situ microscopy: A perspective for industrial bioethanol production monitoring. *Journal of microbiological methods*. **93** (3), 224-232 (2013).
- Havlik, I. *et al.* Monitoring of microalgal cultivations with on-line, flow-through microscopy. *Algal Research*. **2** (3), 253-257 (2013).
- Suhr, H., Herkommer, A. M. In situ microscopy using adjustment-free optics. *Journal of biomedical optics*. **20** (11), 116007-116007 (2015).
- Panckow, R. P., Reinecke, L., Cuellar, M. C., Maaß, S. Photo-Optical In-Situ Measurement of Drop Size Distributions: Applications in Research and Industry. *Oil Gas Sci. Technol. - Rev. IFP Energies nouvelles*. **72** (3), 14 (2017).
- Marbà-Ardébol, A.-M., Emmerich, J., Neubauer, P., Junne, S. Single-cell-based monitoring of fatty acid accumulation in *Cryptocodium cohnii*. with three-dimensional holographic and *in situ*. microscopy. *Process Biochemistry*. **52** 223-232 (2017).
- Porro, D., Vai, M., Vanoni, M., Alberghina, L., Hatzis, C. Analysis and modeling of growing budding yeast populations at the single cell level. *Cytometry. Part A : the journal of the International Society for Analytical Cytology*. **75** (2), 114-120 (2009).
- Brauer, M. J. *et al.* Coordination of growth rate, cell cycle, stress response, and metabolic activity in yeast. *Molecular biology of the cell*. **19** (1), 352-367 (2008).
- Puxbaum, V., Gasser, B., Mattanovich, D. The bud tip is the cellular hot spot of protein secretion in yeasts. *Applied microbiology and biotechnology*. **100** (18), 8159-8168 (2016).
- Marbà-Ardébol, A. M., Emmerich, J., Neubauer, P., Junne, S. in *13. Dresdner Sensor-Symposium 201*. Vol. P2. Prozessmesstechnik 222 - 225 Hotel Elbflorenz, Dresden, (2017).
- Marbà-Ardébol, A.-M., Emmerich, J., Muthig, M., Neubauer, P., Junne, S. Real-time monitoring of the budding index in *Saccharomyces cerevisiae*. batch cultivations with *in situ*. microscopy. *Microbial cell factories*. **17** (1), 73 (2018).



16. Marquard, D., Schneider-Barthold, C., Düsterloh, S., Scheper, T., Lindner, P. Online monitoring of cell concentration in high cell density *Escherichia coli* cultivations using *in situ* Microscopy. *Journal of biotechnology*. **259** 83-85 (2017).
17. Marquard, D. *et al.* In situ microscopy for online monitoring of cell concentration in *Pichia pastoris* cultivations. *Journal of biotechnology*. **234** 90-98 (2016).
18. Camisard, V., Brienne, J., Baussart, H., Hammann, J., Suhr, H. Inline characterization of cell concentration and cell volume in agitated bioreactors using *in situ* microscopy: application to volume variation induced by osmotic stress. *Biotechnology and bioengineering*. **78** (1), 73-80 (2002).
19. Böhm, A., Ücker, A., Jäger, T., Ronneberger, O., Falk, T. in *2018 IEEE 15th International Symposium on Biomedical Imaging (ISBI 2018)*. 1225-1229. (2018).
20. Davey, H. M. Life, Death, and In-Between: Meanings and Methods in Microbiology. *Applied and environmental microbiology*. **77** (16), 5571-5576 (2011).
21. Lodolo, E. J., Kock, J. L., Axcell, B. C., Brooks, M. The yeast *Saccharomyces cerevisiae*.-the main character in beer brewing. *FEMS yeast research*. **8** (7), 1018-1036 (2008).
22. Albertin, W. *et al.* Population size drives industrial *Saccharomyces cerevisiae* alcoholic fermentation and is under genetic control. *Applied and environmental microbiology*. **77** (8), 2772-2784 (2011).
23. Gomes, J., Chopda, V. R., Rathore, A. S. Integrating systems analysis and control for implementing process analytical technology in bioprocess development. *Journal of Chemical Technology and Biotechnology*. **90** (4), 583-589 (2015).